Tellus (2000), 52B, 843–867
Printed in UK. All rights reserved

TELLUS
ISSN 0280–6509

CCN measurements during ACE-2 and their relationship to cloud microphysical properties

By P. Y. CHUANG[1], D. R. COLLINS[1], H. PAWLOWSKA[2], J. R. SNIDER[3], H. H. JONSSON[4], J. L. BRENGUIER[2], RICHARD C. FLAGAN[1] and JOHN H. SEINFELD[1]*, [1]*California Institute of Technology, Pasadena, CA, USA;* [2]*Centre National de Recherches Météorologiques, Toulouse, France;* [3]*University of Wyoming, Laramie, WY, USA;* [4]*Naval Postgraduate School, Monterey, CA, USA*

(Manuscript received 21 January 1999; in final form 21 September 1999)

ABSTRACT

Measurements of cloud condensation nuclei (CCN) concentration at 0.1% supersaturation were made onboard the CIRPAS *Pelican* over the northeast Atlantic during June and July, 1997, in the vicinity of Tenerife, Spain, as part of the second Aerosol Characterization Experiment (ACE-2). The average CCN concentration (N_{ccn}) in the marine boundary layer for clean air masses was 27 ± 8 and $42 \pm 14\ cm^{-3}$ for cloudy and clear conditions, respectively, consistent with measurements made near the British Isles and close to Tasmania, Australia, during ACE-1 for similar conditions. A local CCN closure experiment was conducted. Measured N_{ccn} is compared with predictions based on aerosol number size distributions and size-resolved chemical composition profiles determined from measurements and the literature. A sublinear relationship between measured and predicted N_{ccn}, $N_{ccn} \sim N_{ccn,predicted}^{0.51}$, was found. This result is consistent with some previous studies, but others have obtained results much closer to the expected 1:1 relationship between measured and predicted N_{ccn}. A large variability between measured and predicted N_{ccn} was also observed, leading to the conclusion that, for 95% of the data, the predictions agree with measurements to within a factor of 11. Relationships between below-cloud N_{ccn} and aerosol accumulation mode concentration, and in-cloud cloud droplet number concentration, measured onboard the *Pelican* and the Météo-France *Merlin*-IV, respectively, are calculated for periods while the 2 aircraft were in close proximity at approximately the same time. Measured relationships are reproduced by an adiabatic parcel model, and are also consistent with some previous studies. However, the shape of the CCN spectrum, or the aerosol size distribution, and the updraft velocity are predicted by the model to affect these relationships to a significant extent. Therefore, parameterizations of cloud microphysical properties need to include these variables to accurately predict cloud droplet number concentration. A relationship between N_{ccn} and cloud droplet effective diameter is also calculated and shown to be consistent both with the literature and with the parameterization of effective diameter proposed by Martin et al.

1. Introduction

Clouds are an important component of the climate system. They reflect incoming sunlight, absorb outgoing longwave radiation, and are one of the controlling factors in regulating the tropospheric content of water vapor, an important greenhouse gas. Clouds produce precipitation, a crucial element in climate. Precipitation also plays a role in determining cloud lifetime, in the cycling and ultimate removal of atmospheric aerosols, and possibly in the creation of new particles in the

* Corresponding author address: Department of Chemical Engineering, Mail Code 104-44 Caltech, Pasadena, CA 91125, USA. e-mail: seinfeld@its.caltech.edu

troposphere. Chemical processes that occur within cloud droplets, such as the production of sulfate from SO_2, are also climatically important. Accurately predicting climate change requires an improved understanding of clouds, their influences of climate, and their reaction to changes in atmospheric composition.

To predict climate change, we must understand how anthropogenic aerosol perturbs cloud properties on a global scale. Specifically, it is necessary to understand how cloud properties change as aerosol properties change, i.e., d(cloud property)/d(aerosol property). Cloud albedo is one important climate-related cloud property; it is thought that increases in the concentration of atmospheric aerosol, or more specifically, that subset of atmospheric aerosol upon which cloud droplets nucleate, termed cloud condensation nuclei or CCN, may cause an increase in globally-averaged albedo. It is estimated that such an increase, the so-called indirect climatic effect of aerosols, could alter the global radiation budget to an extent similar in magnitude, but opposite in sign, to greenhouse gas forcing (IPCC, 1996).

In this work, we focus on two major questions, both relating to marine stratus clouds. Such clouds are believed to be climatically the most important due to their frequency of occurrence and extent, and because their albedo and persistence are thought to be sensitive to changes in cloud droplet concentration (Charlson et al., 1992). The first question is whether closure can be achieved for simultaneous measurements of aerosol size distribution and chemical composition, and measured CCN concentration. Köhler theory tells us that, if the aerosol size distribution and chemical composition are perfectly known, then the CCN spectrum is exactly derivable. Several studies (Bigg, 1986; Raga and Jonas, 1995; Hegg et al., 1996; Liu et al., 1996; Covert et al., 1998) have examined the validity of this theory by performing a "local CCN closure" experiment, with widely varying results. A closure experiment is one where a property is measured (in this case CCN concentration at one supersaturation) and compared with results derived using independently measured data (in this case aerosol number size distributions and chemical composition). Closure is achieved if the compared data agree within well-established experimental error. We will address the question of local CCN closure using data from a variety of conditions during ACE-2 and compare the results with those of past studies. CCN closure would provide confidence in our understanding of the aerosol properties that are relevant to CCN, in our measurement of CCN, and therefore in our use of the CCN spectrum as a controlling variable for microphysical cloud models and parameterizations.

The albedo of a warm cloud is, to first order, determined by the cloud droplet number size distribution, which describes the number concentration of cloud droplets as a function of size, and the cloud depth h. It is commonly (but approximately) assumed that, for the purposes of calculating cloud albedo, this distribution can be sufficiently well described by three parameters: the number concentration of cloud droplets, N_{cd}; the cloud droplet effective diameter, D_{eff}, defined as the ratio of the total droplet volume to the total droplet surface area; and the liquid water content, LWC. Using this parameterization, the optical depth τ_c of a spatially uniform cloud is (Twomey, 1977; Seinfeld and Pandis, 1998):

$$\tau_c \simeq \frac{1}{2}\pi h N_{cd} D_{eff}^2.$$

Cloud albedo R_c can then be approximated by:

$$R_c = \frac{\tau_c}{\tau_c + 7.7}.$$

The extent to which the number concentration of CCN, N_{ccn}, and the aerosol number size distribution (or more specifically for this work the accumulation mode particle concentration, N_{ap}, defined as those particles with $D_p(\text{dry}) > 0.1\ \mu\text{m}$) are related to cloud microphysical properties, specifically N_{cd} and D_{eff}, is the second question addressed in this work. Parameterizations of cloud processes used in climate models currently rely on such relationships to predict cloud properties such as albedo. Identifying the variables that control N_{cd} and D_{eff} is critical for developing physically-based parameterizations that reflect atmospheric processes and therefore are predictive. If N_{ccn} and N_{ap} are not the only significant factors influencing N_{cd} and D_{eff}, what other variables are relevant? Measurements from ACE-2 will be used to examine these questions and the results will be compared to those in the literature. Changes in LWC will not be studied as it is thought that total liquid water content is determined predominantly by

large-scale processes rather than microphysical variables.

2. Instrumentation

During the ACE-2 field campaign, the Tenerife-based CIRPAS *Pelican* (Bluth et al., 1996) flew a number of missions, both alone and coordinated with other aircraft, in support of the CLEARCOLUMN, LAGRANGIAN, and CLOUDYCOLUMN experiments. Of specific interest in the present work are the four flights supporting the CLOUDYCOLUMN experiment (Brenguier et al., 2000) during which the *Pelican* flew below stratus cloud decks while the Météo-France *Merlin*-IV flew primarily within the cloud deck. Because the *Pelican's* speed is slower (~ 60 m s^{-1}) and its flight duration longer (~ 12 h) than that of the *Merlin* (~ 90–120 m s^{-1}, ~ 6 h), the 2 aircraft did not fly stacked but rather flew either patterns in the same place but at slightly different times, or non-overlapping patterns that were close to each other, as can be seen in Fig. 1. The flights took place north or northeast of Tenerife. The DLR Dornier-228 also flew above cloud at similar times during these missions measuring cloud radiative properties, but these data will not be discussed here.

The *Pelican* ACE-2 payload included the Caltech CCN instrument which during ACE-2 measured CCN at a fixed supersaturation of 0.1% at a frequency of one measurement approximately every 60 s; the Caltech Automated Classified Aerosol Detector (or ACAD; Russell et al, 1996; Collins et al., 2000) which measures the aerosol size distribution from 0.005 to 0.2 μm at a frequency of one distribution per 45 s using a radial differential mobility analyzer (or DMA; Zhang et al., 1995); a wing-mounted Particle Measuring Systems PCASP-100X optical particle counter measuring the aerosol size distribution from 0.1 μm to 3 μm; and meteorological data measurements such as temperature, pressure, and relative humidity. A wing-mounted Particle Measuring Systems FSSP-100 was also onboard the *Pelican* but stopped working on 4 July, so FSSP data are not available for the CLOUDYCOLUMN flights which all occurred after 4 July. The ACAD and PCASP data are combined to produce aerosol size distributions from 0.005 to 3 μm (Collins et al., 2000). The CCN instrument and ACAD were both located inside the *Pelican* nose and sampled aerosol through a common inlet which had three identical cyclones in parallel. The two instruments shared the same inlet line up until the last 0.75 m. The cyclones have a nominal cut-off diameter of 2.5 μm. Both the CCN and ACAD measurements were performed at a temperature slightly above ambient temperature and therefore at an RH slightly below ambient.

The *Merlin* ACE-2 payload included: the University of Wyoming CCN counter (similar to that described in Delene et al. (1998)) which measured CCN concentration every 40 s for 4 different supersaturations (0.2, 0.4, 0.8 and 1.6%) for a CCN spectrum frequency of one every 160 s; the wing-mounted Météo-France Fast FSSP (Brenguier et al., 1998) for high frequency (1 Hz during this experiment) data acquisition of the droplet size distribution between 2 and 33 μm; liquid water content using a Gerber PVM 100 probe and a PMS King probe; and meteorological data.

2.1. CCN instrument

The Caltech CCN instrument was designed to operate as a CCN spectrometer during ACE-2, i.e., to produce CCN number concentration as a function of supersaturation. However, during post-processing of the data, several factors were identified that limited stability and resolution of the instrument during its initial field deployment. Although these problems limit our ability to invert the raw data to produce CCN spectra for the ACE-2 data set, the instrument can reliably be considered as a fixed 0.1% supersaturation CCN counter for these flights.

The instrument is based on an original design by Hoppel et al. (1979). The Hoppel et al. instrument (originally tended as a condensation nuclei counter) was built using a wet-wall cylindrical column with alternating segments along the column length maintained at warm or cool temperatures to generate a supersaturation profile. The Caltech CCN instrument uses the same principle: a vertically-oriented wet-walled cylindrical tube is axially divided into 14 sections of alternating "hot" and "cold" temperatures. The sample air flows from the top to the bottom of the column. By saturating the air stream at the hot temper-

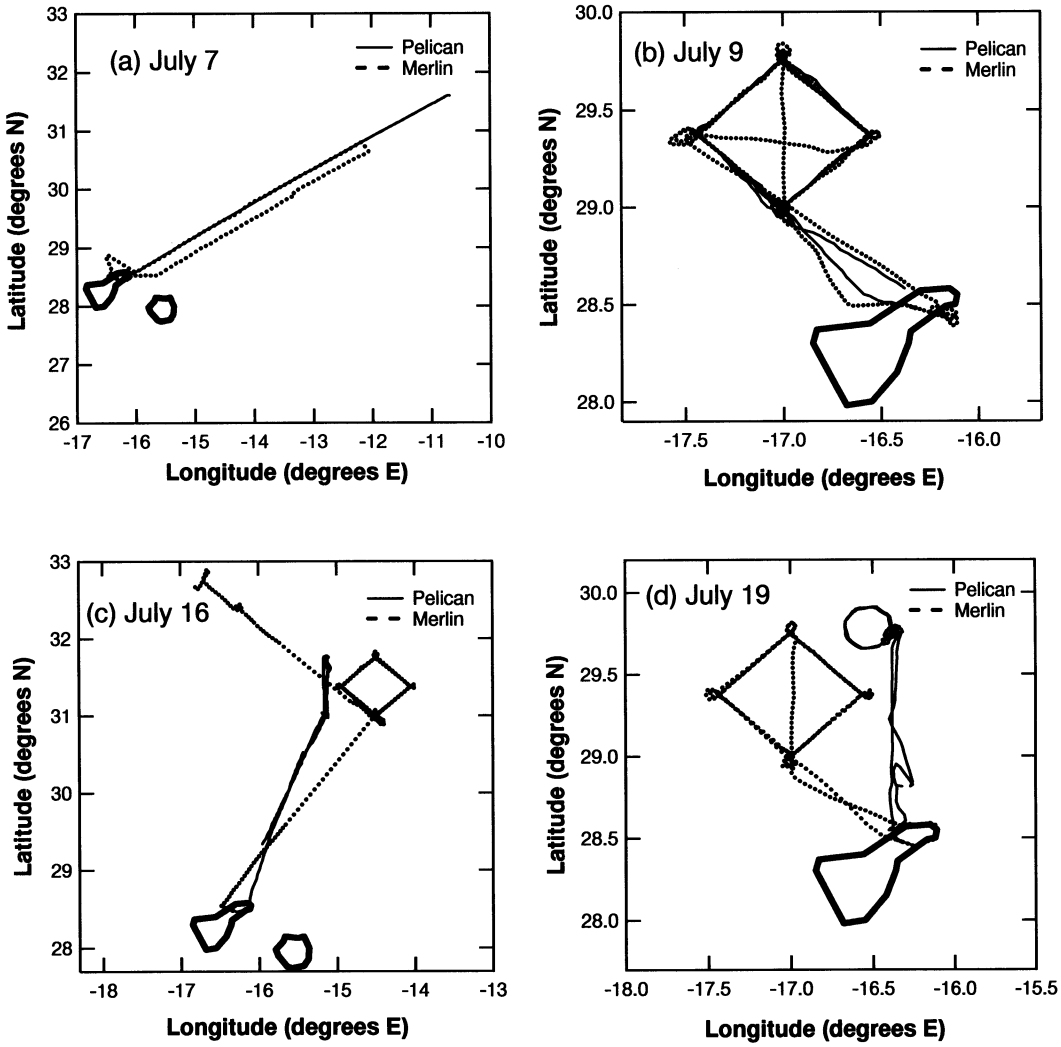

Fig. 1. Flights tracks for the *Pelican* and *Merlin* (with times, in UTC, during which each was in the experimental area) for (a) 7 July (Pelican: 1122 to 1510; Merlin: 1244 to 1408), (b) 9 July (1255 to 1719; 1230 to 1501), (c) 16 July (1338 to 1515; 1323 to 1452), and (d) 19 July (1158 to 1347; 933 to 1131). The *Pelican* return flight track for 7 July is superimposed on the outgoing leg. Flight track data are not complete for 16 July, but the period relevant to this study is shown.

ature, and then exposing it to the cold temperature, a supersaturation that is maximum on the centerline is generated. By increasing the difference in temperature between the hot and cold sections, and by carefully choosing the flow rate, the aerosol sample is exposed to a supersaturation profile that on average is increasing.

This supersaturation profile leads to activation of those particles with lower critical supersaturation (S_c) earlier than those with higher S_c, which allows the lower S_c CCN a longer time to grow within the wetted column. This creates a situation in which CCN with lower values of S_c can be discriminated from those with higher values of S_c by virtue of having grown larger. Therefore, the droplet size at the column exit, which is optically measured, can be related to the critical supersaturation for each particle (Hudson, 1989).

In contrast to a number of CCN counters for which calibration is thought not to be an inherent requirement, calibration of the device is needed to establish the relationship between outlet diameter and S_c.

A specially designed optical particle counter (OPC) was used to measure droplet diameter at the exit of the CCN growth column. It measures the total laser (670 nm) light scattered from each droplet in the near forward direction. This light scattering measurement has been optimized through theoretical and laboratory studies to produce a nearly monotonic response from water droplets 0.7 to 20 μm in diameter. The scatter light pulses from individual particles are converted to a voltage signal using a photomultiplier tube. The peak intensity of each voltage pulse, which corresponds to droplet diameter, is then measured and binned by a multichannel analyzer (MCA), which has 2048 channels from 5 mV to 10 V.

Laboratory calibrations of the CCN counter were performed before and after ACE-2, and field calibrations were performed during the experiment. The instrument was calibrated by generating a nearly monodisperse salt aerosol (amonium sulfate for laboratory experiments, sodium chloride in the field) by atomizing a salt water solution, drying the resulting aerosol, and selecting those particles within a narrow size range using a differential mobility analyzer. For the purposes of the single supersaturation instrument used for this study, the important result is that for particles whose size is calculated to correspond to 0.1% supersaturation, the channel in the MCA at which the response is maximum is reasonably constant over all calibrations. From this calibration, it is assumed that all droplets larger than this threshold diameter are CCN with critical supersaturations below 0.1%. The effect of changes in this threshold channel has been investigated and found to result in a negligibly small change in the measured CCN concentrations relative to instrumental error for the data considered here. Expected changes in this threshold channel, as measured in 21 laboratory calibration experiments conducted over the course of 9 months, are calculated to result in errors in each data point of less than 5%, 90% of the time.

2.2. *Instrument intercomparison*

To validate the CCN instrument performance we compare the instrument response against that of other CCN counters for a common aerosol sample. During ACE-2, there were a number of opportunities for such comparisons, mostly with the *Merlin* CCN instrument but also with a similar instrument onboard the MRF C130. Both of these instruments are classic static thermal diffusion CCN counters (Twomey, 1963). For the C130, there was a 15 min period on 14 July during which the two aircraft flew in close proximity at the same altitude. During this interval, the Caltech and MRF instruments measured N_{ccn} values of 57 cm^{-3} and 47 cm^{-3} at 0.1% supersaturation, respectively.

To estimate CCN concentrations at 0.1% supersaturation from the *Merlin* CCN counter, the CCN spectrum is assumed to follow the parameterization $N_{ccn} = CS^k$ (where S is supersaturation and C and k are fitting parameters). Using the values of N_{ccn} measured at 0.2 and 0.4% supersaturation, the two fitting parameters C and k are determined, from which N_{ccn} at 0.1% is then calculated by using this parameterization. Examination of CCN spectra measured from the CCN instrument onboard the MRF C130 (which measured CCN concentration at five different supersaturations, 0.1, 0.2, 0.4, 0.6, and 1.0%) during ACE-2 show that this assumption is likely to be reasonable. For 70% of the cases during ACE-2, CCN concentration at 0.1% supersaturation measured by the MRF instrument agrees well (within about 20%) with that concentration extrapolated from the MRF CCN concentrations measured at 0.2 and 0.4% supersaturation. For the remaining cases, the number of spectra for which this assumption is an over-estimate of CCN concentration appears roughly equal to the number of spectra for which the opposite is true.

A number of opportunities existed for intercomparison of the *Merlin* and *Pelican* CCN instruments; during four periods the *Merlin* and *Pelican* were in close proximity for an extended time. The results from these direct comparison intervals are presented in Fig. 2 (squares). There are also a number of longer periods over 6 flights for which both the *Merlin* and *Pelican* were sampling below cloud at about the same place and time (Fig. 2, circles). It can be seen that in general the intercomparison agreement is good. The ratio of *Merlin* to *Pelican* CCN concentration averaged over all flights (except those where the data can be reasonably neglected as discussed below) is 1.15 ± 0.15

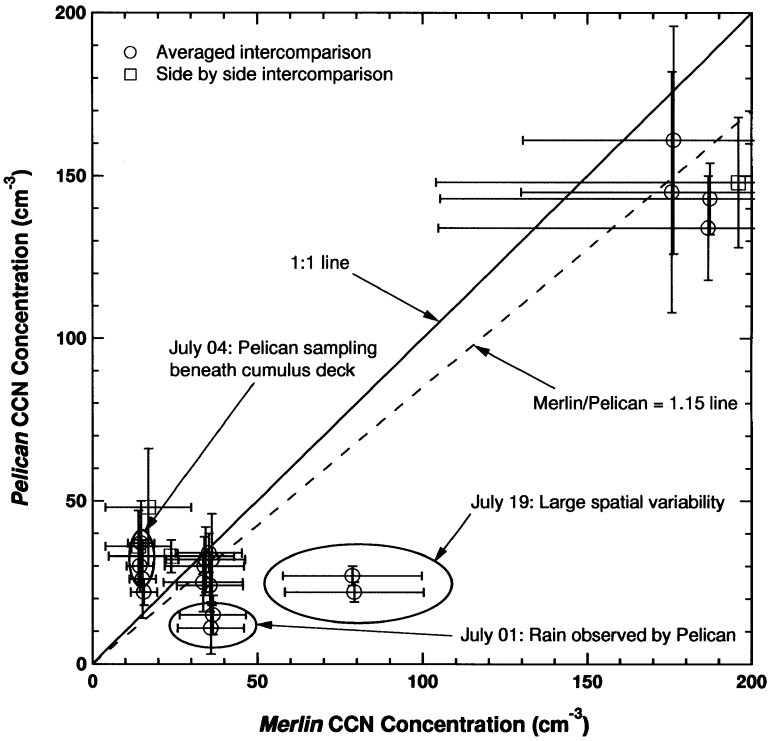

Fig. 2. Intercomparison of *Pelican* and *Merlin* CCN instruments at 0.1% supersaturation. Circled data are those that were discarded because of the problems labelled here and discussed in the text. The "*Merlin*/*Pelican* = 1.15 line" is plotted because the average ratio of *Merlin* to *Pelican* CCN concentrations is 1.15 ± 0.15 (1 σ). The data labelled "Averaged intercomparison" (circles) are those data for which the *Merlin* and *Pelican* were in the same vicinity at similar, but not identical, times. The data labelled "side by side intercomparison" (squares) are those data for which the *Merlin* and *Pelican* were simultaneously flying next to each other.

(1σ). For 1 July, the two *Pelican* measurements with very low concentrations (11 and 15 cm^{-3}) may be a result of rain that was observed in the flight path. On 4 July, the concentrations observed by the *Pelican* appear to be systematically higher than those observed by the *Merlin*. This difference may be explained by the fact that the first three legs of the *Pelican* flight were performed beneath a cumulus layer that was present below the stratus cloud deck. The significantly lower concentration measured during the fourth *Pelican* leg that was flown between the cumulus and stratus layers where the *Merlin* was sampling agrees more closely with the *Merlin* data. On 19 July, the *Pelican* and *Merlin* flew adjacent patterns (Fig. 1). The *Merlin* time series shows a strong gradient in CCN concentration, with the air being significantly cleaner towards the north and east where the *Pelican* was flying. It is possible, then, that this could help explain the large discrepancy between the *Pelican*, measuring clean conditions, and the *Merlin*, measuring more polluted air.

3. Adiabatic cloud parcel model

An adiabatic cloud parcel model developed at Caltech (Nenes et al., submitted to *J. Geophys. Res.*) will be used to aid data evaluation. Model predictions of below-cloud and in-cloud properties of an idealized cloud will be compared with measurements. Consistency between predicted and measured relationships provides experimental verification of our theoretical understanding of the underlying physical processes that give rise to these relationships. Differences between the

observed and predicted trends suggest that either the measurements need to be improved, or the model does not accurately describe the physical system, or both. Potential measurement problems include: biasing of the data due to non-isokinetic sampling or droplet shatter; incorrect assumptions about particle refractive index leading to incorrect inversion of optical particle counter data; and changes in the supersaturation profile in CCN instruments due to problems with water delivery. Model predictions could be inaccurate if processes that are not included in the model, such as turbulence, coalescence, and uptake of soluble gases,a are important.

Nenes et al. compare the Caltech model with a similar but independent model developed at Texas A&M; the models yield very similar results for identical input conditions. Both models are based on the dynamic Köhler theory as described by, for example, Seinfeld and Pandis (1998). Entrainment was neglected for the simulations presented in this study. Nenes et al. used two aerosol size distribution/chemical composition profiles that are relevant to the present study (Fig. 3). The first, labelled D1, is a size distribution

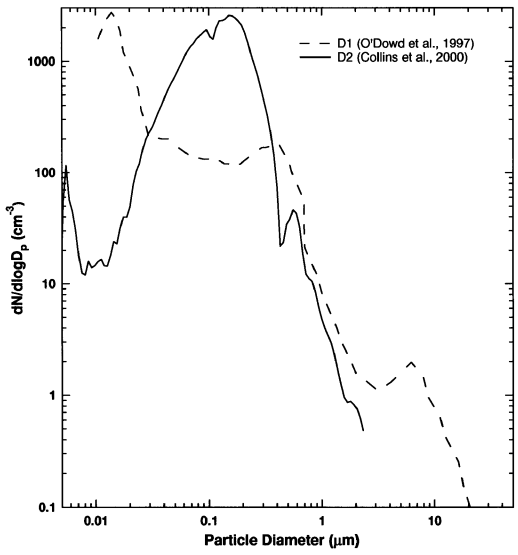

Fig. 3. Size distributions D1 and D2 used for adiabatic parcel model calculations. D1 is representative of clean marine conditions and obtained from O'Dowd et al. (1997). D2 is representative of polluted marine conditions in the northeast Atlantic as measured during ACE-2 (Collins et al., 2000).

from O'Dowd et al. (1997) characteristic of clean marine conditions. The chemical composition was assumed to be predominantly ammonium bisulfate for particles with $D_p < 1$ μm, and predominantly sodium chloride for larger particles. The second size distribution, labelled D2, is obtained from ACE-2 size distribution measurements from the *Pelican* (Collins et al., 2000) for polluted marine conditions. This aerosol was assumed to be composed solely of ammonium sulfate. Both distributions, were used, however, as model inputs under both clean and polluted conditions, by scaling the total number of aerosol particles but not changing the shape of the aerosol size distribution, in order to evaluate the effect of different size distribution shapes on predicted cloud properties. A value for the mass accommodation coefficient of 1.0 was chosen for all calculations.

4. Results and discussion

4.1. CCN measurements

Table 1 summarizes CCN concentrations and their standard deviations measured in the marine boundary layer (MBL) during ACE-2. The standard deviations are those calculated from all the CCN concentration data (60 s per datum) available for each interval. Broadly, there are four different conditions during which CCN measurements were made, categorized by two factors: whether the air is clean or polluted; and whether the local conditions are clear or cloudy. Results are reported only for the MBL, which was characterized by high relative humidity (RH). The difference in RH between the free troposphere and the MBL is normally quite large (typically $<30\%$ for the free troposphere versus $>70\%$ for the boundary layer) and quite sharp, so it is straightforward to distinguish between these environments.

CCN number concentrations from the clean cases can be compared with previous relevant studies. Measurements during ACE-1 over the southern Pacific in the vicinity of Tasmania reported by Hudson et al. (1998) show average CCN concentrations at 0.1% to be roughly 35 cm^{-3} for cloudy conditions, and 50 cm^{-3} for clear conditions. These values are similar to the present data, 27 ± 8 and 42 ± 14 cm^{-3}. The average Northern Hemisphere CCN concentration might be expected to exceed that for the Southern

Table 1. *Summary of CCN concentrations measured by the Pelican during ACE-2 as a function of conditions*

Conditions	Date	Flt #	Alt (m)	# Data pts.	N_{ccn} (cm^{-3})	σ (cm^{-3})
clear, clean	July 10	17	92	8	28	6
	July 08	15	57	6	29	4
	July 05	12	1260	29	34	6
	July 30	8	46	17	43	21
	July 05	12	189	28	45	10
	July 05	12	28	31	46	16
	July 05	12	743	28	48	14
average:				147 total	42	14
clear, polluted	July 17	20	61	11	82	13
	July 10	17	88	15	144	49
	July 10	17	650	18	282	85
	July 17	20	645	14	526	103
average:				58 total	267	180
cloudy, clean	July 19	22	509	29	22	3
	July 16	19	20	29	25	9
	July 19	22	44	30	27	3
	July 16	19	50	21	30	9
	July 16	19	37	28	32	10
average:				109 total	27	8
cloudy, polluted	July 18	21	184	26	63	25
	July 18	21	612	26	70	14
	July 18	21	58	28	79	37
	July 18	21	182	25	97	33
	July 18	21	56	24	111	31
	July 18	21	605	25	127	13
	July 09	16	458	65	134	16
	July 09	16	183	59	143	10
	July 07	14	203	67	145	37
	July 07	14	296	59	161	34
	July 09	16	184	9	198	8
	July 09	16	456	10	202	11
average:				423 total	128	43

Hemisphere because of anthropogenic influences, but, at least for these two snapshots of data, this expectation is not supported. This finding may not be surprising because back trajectories (not shown) for the clean cases reveal that these air particles had not come close to continents for at least five days, and perhaps longer, such that much of the anthropogenic aerosol should have been removed by the time the air mass was sampled. MBL CCN concentrations were observed to be lower under cloudy conditions than under clear conditions during both studies. The ratios of cloudy to clear CCN concentrations, 0.70 for Hudson and 0.64 in this study, are also quite consistent. This observation might be explained as follows. CCN in a below-cloud air parcel are advected upward and, upon entering the cloud, activate to form large droplets. These droplets coalesce very slowly due to their low diffusivities, but collisions with other droplets due to differential settling or turbulent mixing may reduce the number concentration of droplets in the cloud. When the air parcel subsequently advects downwards and out of the cloud, causing the cloud droplets to evaporate, the total number of CCN is lower. Another possibility is the removal of

cloud droplets by precipitation, which would also cause a decrease in CCN number in an air mass that was recently in-cloud. Further discussion of this issue can be found in Twomey and Wojciechowski (1969) and Hudson and Frisbie (1991).

Raga and Jonas (1995) report CCN measurements onboard the MRF C130 over the British Isles on 7 May 1992 when "relatively clean conditions" were encountered within a cloud-topped boundary layer. Average CCN concentrations at 0.1% supersaturation of 25, 35, and 50 cm^{-3} (average = 37 cm^{-3}) were found at three different altitudes within the boundary layer (1050, 1500, and 60 m respectively). These values are also similar to the clean cloudy condition average of 27 ± 8 cm^{-3} measured here. Lastly, an average of 30 cm^{-3} has been reported as the Cape Grim historical average for the months November and December (which is roughly the same reason as for ACE-2 except in the Southern Hemispehre) for the years 1987 to 1993 (Covert et al., 1998). Cape Grim is a remote coastal site in northwest Tasmania that often experiences very clean air. To estimate CCN concentrations at 0.1% supersaturation from the Cape Grim and MRF data, the averaged measured spectra were extrapolated from the lowest two supersaturation values (approx. 0.5 and 0.2%; and 0.45 and 0.2%, respectively) to 0.1% using the parameterization $N_{ccn} = CS^k$ that, as described above (Section 2.2), is likely to yield reasonable estimates.

4.2. *Past studies of simultaneous CCN and aerosol measurements*

As discussed above, it is generally assumed that, if the number size distribution and chemical composition of an aerosol is perfectly known, then we can predict exactly the CCN spectrum. It is often further assumed that for determining the critical supersaturation of an aerosol particle, i.e., that supersaturation at which that particle activates, only two parameters are important: the number of moles of solution-phase species in the particle, and the volume of insoluble material present. This CCN model can be tested using CCN closure experiments, in which CCN concentration predicted using measured aerosol size distributions, and chemical compositions that are either assumed or derived from experimental data, are compared with simultaneous CCN measurement. It is important to note that achieving such CCN closure implies that we understand the processes that govern CCN activation in the CCN instrument. It does not imply that we fully understand how CCN activate and grow in actual clouds, as there are several factors that may be relevant in real clouds that CCN instruments do not accurately reproduce at present, e.g., the kinetics of cloud droplet activation (Chuang et al., 1997), the presence of soluble gases (Laaksonen et al., 1998), and the time profile of supersaturation that an aerosol particle experiences, which is influenced by cloud dynamical processes such as entrainment, and by cloud microphysical factors such as the total CCN concentration. An inability to achieve closure could imply that the traditional Köhler theory used to predict CCN concentration measurement data requires additional variables not previously considered in order to accurately do so, or alternately that the CCN concentration, aerosol size distribution, and/or chemical composition measurements require improvement for the purpose of closure experiments. A number of previous studies that have examined local CCN closure are summarized in Fig. 4 and are discussed in more detail below.

Bigg (1986) compared predicted and measured CCN for a wide range of CCN concentrations at Cape Grim, Australia. Predicted CCN concentration was based on measured size distributions and the assumption that the particles were composed solely of either sodium chloride or ammonium sulfate. For all five supersaturations (ranging from 0.25 to 1.25%), the agreement between predicted and measured CCN concentrations was substantially better for low concentrations. The ratio of measured to predicted N_{ccn} at 0.25% assuming the aerosol to consist of solely of sodium chloride, was 0.79, 0.41, and 0.18 for air with particle concentrations of less than 300 cm^{-3}, between 300 and 3000 cm^{-3}, and greater than 3000 cm^{-3}, respectively. Assuming an aerosol composed of ammonium sulfate yields ratios of 1.3, 0.70, and 0.30. Incorporating CCN to CN ratios reported by Gras (1990) for Cape Grim, data at 0.25% supersaturation can be estimated, and are plotted in Fig. 4.

Liu et al. (1996) examined the relationship between CCN measurements at 0.06% supersaturation at a ground site in Nova Scotia, Canada

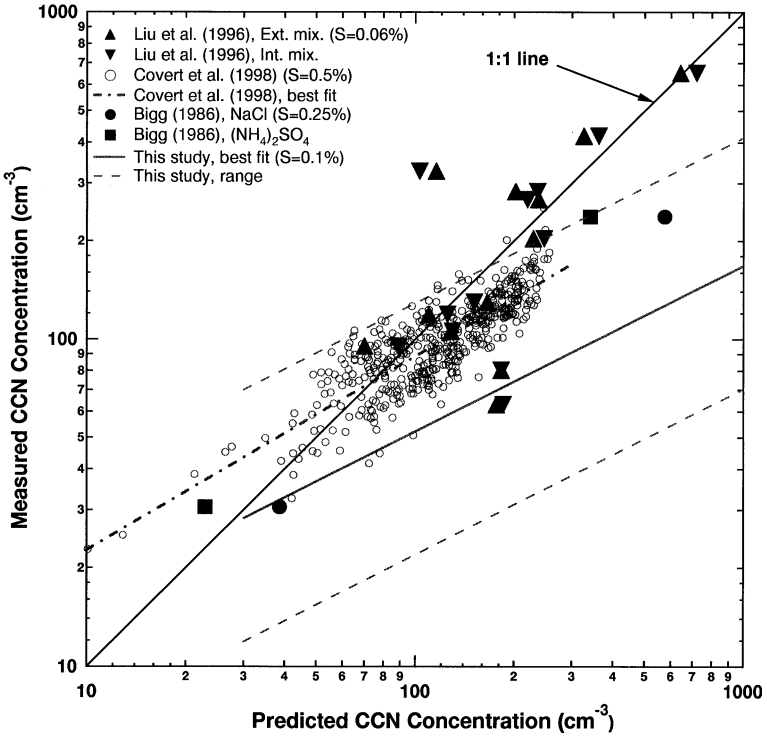

Fig. 4. Results of previous closure experiments, along with those of the current study. The data from the present study are not plotted explicitly for presentation clarity.

using an isothermal haze chamber (Laktionov, 1972), and CCN concentration predictions based on a combination of size distribution measurements (from a PCASP measuring 0.135 to 3.0 μm) and chemical composition data obtained from filter samples. Both internal and external mixture models for aerosol composition were examined. The ratio of measured to predicted CCN concentrations averaged over all data was 0.9 ± 0.3 (1σ). This suggests that closure was achieved on average, although several data points fall well outside of closure agreement even after error bars are estimated. One difference between this study and the others cited is the use of an isothermal haze chamber for measuring N_{ccn}. This instrument does not activate droplets but, instead, measures the equilibrium diameter of particles at 100% RH, so factors that are relevant to droplet growth and activation should not affect the isothermal haze chamber measurements to the same extent that they do classic CCN counters. Thus, it is possible that prediction of the 100% RH equilibrium size may be more easily achieved given a size and chemical composition distribution than the CCN activation spectrum.

At the Cape Grim site during the ACE-1 field campaign, Covert et al. (1998) measured the aerosol number size distribution and CCN concentration at 0.5% supersaturation. In addition, they measured hygroscopic growth factors using a tandem DMA (TDMA) system. This method thereby quantitatively differentiates more hygroscopic aerosol from less hygroscopic aerosol, from which information about the chemical composition and aerosol mixing state can be inferred. Covert et al. found that, when predicted N_{ccn} was plotted against measured N_{ccn} without incorporation of the hygroscopic growth data, the correlation coefficient R for a linear straight line fit was 0.71. When the hygroscopic growth data were combined with the size distribution data to predict N_{ccn}, R increased to 0.84. As a result, Covert et al. concluded that the indirect chemical information obtained from the TDMA system was useful for

N_{ccn} prediction because these data explained some of the variability in the plot of predicted to measured N_{ccn}. Physically, the chemical information increases the accuracy of predicting N_{ccn} by excluding that fraction of the aerosol that is unlikely to serve as CCN because of their limited hygroscopic nature, and by improving estimates of the supersaturation at which the CCN activate based on the chemical compositions inferred from the hygroscopic growth rates. The average ratio of measured N_{ccn} to N_{ccn} predicted using TDMA data is 0.79, with 90% of the data lying in the range of ratios from 0.6 to 1.1. However, they also found a systematic over-prediction of N_{ccn} that they could not explain in terms of random instrument error, and as a result, conclude that they could not achieve local closure. The greatest discrepancies appeared to occur for polluted air masses. This result is interesting since previous investigators have assumed that the scatter in a plot of measured versus predicted CCN concentration can be explained by differences in chemical composition and in the mixing state of the aerosol, factors that the TDMA data should take into account.

Further discussion of these local closure experiments follows the next section which addresses the data from the present study.

4.3. *Current study*

The current study uses the *Pelican* CCN and aerosol number size distribution measurements to evaluate the extent to which local CCN closure can be achieved. CCN data are reported every 60 s, whereas the size distribution data are reported every 90 s. The size distribution measurement closest in time is used to compare against each CCN measurement. Size-resolved aerosol chemical composition data were not available at the same spatial and temporal resolution as the size distribution and CCN data. Instead, flight-averaged chemical profiles were estimated from a combination of ground-based filter measurements at Punta del Hidalgo (PDH), Tenerife, and by making assumptions regarding the relative concentrations of the various components. PDH is located at the northern end of Tenerife at an elevation of 30 m. Because northerly winds generally prevail in this region, PDH is assumed to be representative of marine boundary layer air that is undisturbed by the local islands. Major species measured at PDH are NH_4^+, SO_4^{2-}, Na^+, Cl^-, and both elemental and organic carbon (EC and OC, respectively) for both fine ($D_p < 1$ μm) and coarse ($D_p > 1$ μm) aerosol modes (Putaud et al., 2000). Nitrate was also measured and found to be negligible in abundance relative to sulfate and chloride. The distribution of sulfate among H_2SO_4, NH_4HSO_4, and $(NH_4)_2SO_4$ was based on observations of the ammonium to sulfate ratio. Sea salt was assumed to be externally mixed with the sulfate aerosol. EC and OC were assumed to be predominantly internally mixed with sulfate and sea salt aerosol with a small amount externally mixed. Volatility measurements in marine conditions in the North Atlantic (Clarke et al., 1996) showed that a majority of particles contained a non-volatile residual core that was composed partially or entirely of EC, supporting this assumption for EC. While no similar data are available to support the assumption that OC is internally mixed, it is believed that organic aerosol originates predominantly from land sources (Cachier et al., 1986) and generally will have become internally mixed through condensation and coagulation over the several days since the organic compounds were emitted. By combining the PDH measurements and these assumptions, a size-resolved chemical composition profile for each flight is obtained which is consistent with the observed chemical composition at PDH for that time period. Fig. 5 shows sample chemical composition profiles for polluted and clean air. The actual chemical composition profiles used are slightly different for each flight; the relative amounts of sea salt, OC, EC, and the sulfate compounds are adjusted so that the calculated submicron mass composition is the same as that measured at PDH at the same time. The derivation of these chemical composition profiles are discussed in more detail by Collins et al. (2000). Given the ambient size distribution and the derived chemical composition, the dry aerosol size distribution is computed.

A CCN spectrum was then computed based on these size/composition distributions. The predicted CCN concentration was then calculated by summing all CCN predicted to have critical supersaturation less than 0.1%. To do so, it was assumed that: the surface tension of the droplets is that of water; all inorganic salts fully dissociate; and the OC and EC fractions are insoluble. For droplets

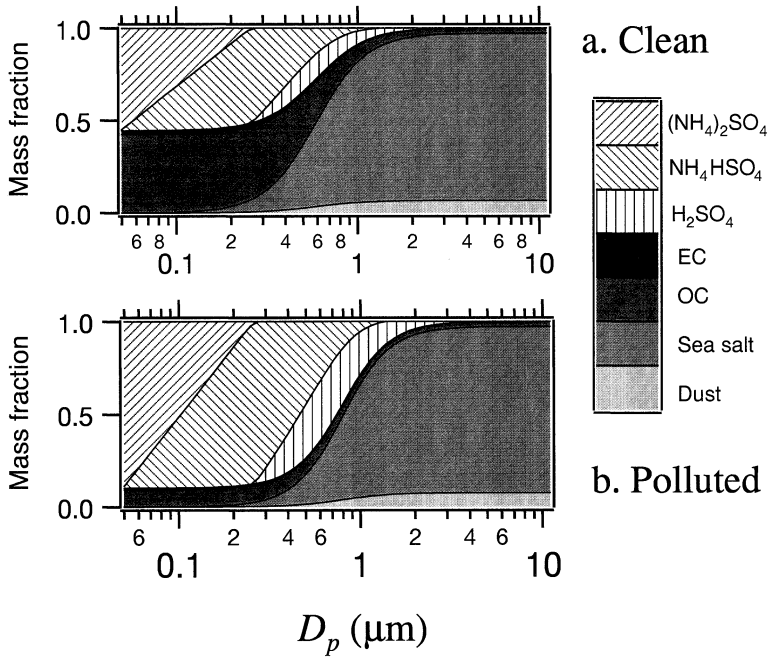

Fig. 5. Sample size-resolved chemical composition profiles for (a) clean and (b) polluted conditions that are used together with aerosol size distribution data to derive CCN spectra (see text).

of sizes close to their critical diameter, the solute concentration is fairly low (order 10 mM) so the surface tension correction is small and the important inorganic species are well below their solubility limit. It is expected that the EC fraction is hydrophobic, but it is likely that the OC fraction is partly water soluble, and partly insoluble. The assumption that OC is insoluble leads to a lower-bound estimate of the CCN concentration at 0.1%, as increasing the amount of soluble species by assuming some of the OC to be water soluble would increase the derived CCN concentration by shifting the CCN spectrum toward lower critical supersaturations.

To estimate the uncertainty in measured CCN concentration, it was assumed that the CCN instrument maintained a supersaturation within $\pm 30\%$ of the mean value of 0.1%. Using the derived CCN spectrum, the number concentration at 0.07%, 0.1%, and 0.13% were calculated. The ratios of CCN concentration at 0.07% to that at 0.1%, and at 0.1% to 0.13% (both ratios >1) were then calculated. These ratios were then used to estimate the relative uncertainty in the measured CCN concentration at 0.1% supersaturation. This method therefore quantitatively calculates instrument uncertainty while accounting for the shape of the CCN spectrum in measuring CCN concentration; if the distribution is very steep, then the ratios will be large and the uncertainty correspondingly large, which is a reasonable expectation.

A total of 684 comparisons of measured and predicted CCN concentrations over nine flights are shown in Fig. 6. The data were taken in the boundary layer during constant altitude legs in both clear and cloudy conditions. While there is considerable scatter, a regression of all data (except data from 8, 10, and 19 July, as explained below) gives the relationship $N_{ccn} \sim N_{ccn,predicted}^{0.51}$, with a 95% confidence interval for the exponent of 0.47 to 0.54, where N_{ccn} and $N_{ccn,predicted}$ are measured and predicted CCN concentration at 0.1% supersaturation, respectively. The large variability observed in Fig. 6 does not appear to originate only from random instrument error. The average instrumental error was measured by relative standard deviation (σ/N_{ccn}) for all N_{ccn} data is 0.22,

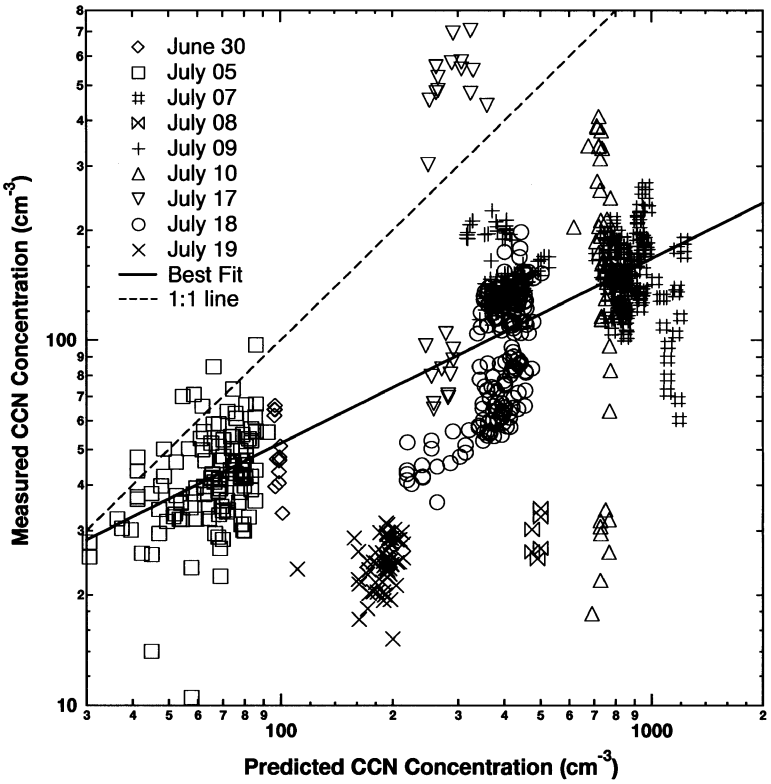

Fig. 6. Local closure of CCN. Plot of measured and predicted number concentration of CCN at 0.1% supersaturation for cloudy (open symbols, e.g. X) and clear (closed symbols, e.g. O) conditions. The best fit line does not include part of the data from 17 July, and also excludes all of the data from 08 and 19 July (see discussion in text). The error bars for each measurement are not shown; the average relative standard deviation (defined by $\sigma/N_{\mathrm{ccn,measured}}$ for the plotted data is 0.22. Error bars for the predicted CCN concentration are estimated to be at most 37% of the predicted value (see text).

with a maximum of 0.49. In comparison, the average ratio of measured to predicted CCN concentration, $F_{\mathrm{ccn}} = N_{\mathrm{ccn}}/N_{\mathrm{ccn,predicted}}$, is 0.34. Therefore, it is unlikely that instrumental random error is the cause of this systematic bias of F_{ccn}. The 2.5 and 97.5 percentile values of F_{ccn} are 0.09 and 0.89 (i.e. 95% of the data falls between 0.09 and 0.89), a difference of a factor of 10. Therefore, we conclude that, for the present study, measured N_{ccn} is on average smaller than predicted N_{ccn} by a factor of 0.34. N_{ccn} predictions are within a factor of 11 ($=1/0.09$) of the measurements 95% of the time.

A different analysis examines the ratio of measured N_{ccn} to that calculated from the best-fit relationship $N_{\mathrm{ccn}} \sim N_{\mathrm{ccn,predicted}}^{0.51}$, which is on average 1.1, with 66% of the values lying between 1.3 and 0.72 (factor of 1.8), and 95% of the values lying in the range 2.1 and 0.42 (factor of 5). In comparison, the 1 σ variability in F_{ccn} with respect to the best-fit relationship due to random error is expected to be a factor of 1.5 ($=(1+0.22)/(1-0.22)$), which is 80% ($=1.5/1.8$) of the observed variability. Thus, we further conclude that 20% of the variations observed with respect to the best-fit relationship are due to factors not considered in the calculation of predicted N_{ccn} in the present study, and that this relationship predicts N_{ccn} to within a factor of 2.4 ($=1/0.42$), 95% of the time.

Data from July 08 (clear conditions with dust layer aloft), 19 July (clean cloudy conditions), and part of 10 July (polluted clear conditions) lie significantly below the best fit line and are possibly

inaccurate. The N_{ccn} data for 19 July were likely affected by an instrument problem. Drying of the CCN column because of a problem in the water delivery system was noted post-flight and is the likely cause of the low CCN concentrations measured. Scaling these data to higher N_{ccn} as suggested from this plot (scaling the data to a mean of around 60 cm^{-3}) improves the agreement of the data relating N_{ccn} with N_{cd} and D_{eff} (described below), which is independent evidence suggestive of an instrument malfunction. The data from 10 July that fell well below the regression line at around $N_{ccn,predicted}$ of 600 cm^{-3} and N_{ccn} of 30 cm^{-3} may also be an instrument artifact, perhaps a result of the change in altitude that occurred just prior to the measurement. The time series (not shown) exhibits a large reduction in N_{ccn} which is not mirrored in the size distribution data. Such responses were not seen for many altitude changes but did occasionally occur. The data from 10 July may also be a result of such problems as there are only a few minutes worth of data at the end of a spiral maneuver. The *Pelican* ascended back into the free troposphere after only a few minutes in the boundary layer so there was no opportunity to observe a relaxation to higher N_{ccn} if it would have happened.

The data from 17 July with very high N_{ccn} correspond to the *Pelican's* flight path crossing the wake of Tenerife. Integrating the size distribution data yields an estimate of the total aerosol number concentration of 13 500 cm^{-3}, reflecting highly anthropogenically-influenced air. Interestingly, these data exhibit F_{ccn} values around 2. It is unclear, however, why the recently-emitted accumulation-mode aerosol in this polluted air mass should exhibit such large ratios of N_{ccn} to $N_{ccn,predicted}$ as compared to the rest of the data set.

An analysis of the sensitivity of $N_{ccn,predicted}$ to the assumed chemical composition profiles was conducted. Base case chemical composition profiles were obtained by adjusting the various amounts of sulfate, sea salt, OC, and EC until the integrated submicron mass matched the submicron composition profile measured at PDH for the same period. The amount of sea salt, OC, and EC were then varied by 50% from their base case values, which is a conservative estimate since the errors associated with the composition measurements are likely to be smaller. Sulfate dominates the measured submicron aerosol mass at PDH (comprising about 75%, with a range of 66 to 80%) and is added or subtracted as the other components are varied to maintain constant total mass. EC makes up very little of the submicron aerosol, on average of 2% by mass, and therefore predicted $N_{ccn,predicted}$ is very insensitive to changes in EC mass. Increasing and decreasing sea salt mass changes $N_{ccn,predicted}$ on average by 4%. This value is very small because sulfate is lost and gained as sea salt is increased and decreased. By mass, sulfate and sea salt result in similar (although not identical) number of moles of solution phase species upon dissolution, which explains the small change in $N_{ccn,predicted}$ despite the large imposed change in composition. Changes in OC mass, which is assumed to be insoluble as discussed above, result in $N_{ccn,predicted}$ changes of 22% on average. Another factor that was examined was whether the aerosol was internally or externally mixed. The average difference in $N_{ccn,predicted}$ between these two extreme mixing states is 15%. Note that the profile that is actually used is somewhere in between the two mixing extremes. Therefore, the typical error of $N_{ccn,predicted}$ with respect to chemical composition is pessimistically estimated to be $15 + 22 = 37\%$. It appears, then, that even large changes in the chemical composition of the aerosol cannot explain fully the variability observed in Fig. 6.

4.4. *Local CCN closure: discussion*

The studies by Bigg (1986), Covert et al. (1998), and the present study (Fig. 4) suggest that the relationship between measured and predicted N_{ccn} is sublinear, i.e., that the ratio of measured and predicted N_{ccn} decreases as predicted N_{ccn} increases. Such a relationship does not correspond with proper CCN closure. However, these three studies either assume the chemical composition of the aerosol (Bigg) or infer chemical composition indirectly (Covert et al. and present study) and therefore the measurements are not ideal for examining CCN closure. Covert et al. (1998) use TDMA measurements to infer the aerosol mixing state and chemical composition. While they are close to achieving CCN closure, they conclude that the systematic discrepancy between predicted and measured N_{ccn} is real. Only the study by Liu et al. (1996) appears to achieve CCN closure, and even then, three of 11 cases show large deviations from

a 1 to 1 relationship. Whether this discrepancy is a result of instrument malfunction, air mass characteristics, or other factors is unclear. The isothermal haze chamber Liu et al. used to measure CCN may explain their ability to achieve closure since CCN activation does not occur in such an instrument. Additional studies in CCN closure in a variety of conditions is required before this issue can be definitively settled.

If a sublinear relationship between measured and predicted N_{ccn} does exist, one possible explanation is depletion of water vapor within a CCN instrument. Given a sufficiently high aerosol loading, all CCN counters will experience a decrease in the supersaturation available for growth when the amount of water condensed onto particles becomes a significant fraction of the available water vapor. This would explain decreases in measured N_{ccn} for increasing predicted N_{ccn}. However, it appears that the static diffusion cloud chambers used by Bigg (1986), and Covert et al. (1998) do not experience significant water vapor depletion for CCN concentrations below a CCN concentration of 2000 cm^{-3} (Delene et al., 1998), well above the concentration at which the sublinear relationship is observed.

The amount of insoluble material is often considered to be a free variable that is inferred from discrepancies between CCN measurements and predictions (Hegg et al. (1991), Raga and Jonas (1995)). In this study, the measured insoluble material is very small (less than 3% of the total submicron aerosol mass), and therefore cannot explain the lack of closure.

The presence of organic species in the aerosol in increasing amounts as aerosol concentrations increase is another possible explanation of a sublinear relationship between N_{ccn} and N_{ap}, since polluted air masses tend to contain greater quantities of organic compounds than clean air masses. It is known that organics can modify the traditional Köhler curve by altering the droplet surface tension, by exhibiting slightly soluble behavior (Shulman et al., 1996), and possibly by other mechanisms such as changes in the mass accommodation coefficient. Impeded droplet growth due to organic coatings has been hypothesized to explain observations of delayed droplet growth in static thermal diffusion CCN instruments (Bigg, 1986). Kinetic inhibition of CCN activation in CCN instruments due to the presence of organics could also further decrease measured N_{ccn} (Chuang et al., 1997), especially under conditions of high N_{ap}. Such modifications to traditional Köhler theory would change the calculation of the CCN spectrum which would therefore alter predicted CCN concentrations. In the present study, however, the relative abundance of organic compounds is higher for clean air masses than for polluted ones (although polluted air masses have more total mass of OC). It is possible that these effects are caused only by those organic species formed from anthropogenic sources and not from naturally occurring ones, thereby causing the observed sublinear behavior. Without detailed organic speciation data in conjunction with the other measurements necessary for local closure, the effect of organics on CCN remains an open question.

4.5. *Below cloud CCN concentration versus cloud properties*

Cloud properties depend on a number of variables, some microphysical and others of larger scale. Microphysical parameters include the CCN spectrum, which is related to the aerosol number size distribution and chemical composition. Larger scale variables such as updraft velocity, cloud thickness, and turbulent mixing. The following sections discuss the relationship between measured CCN concentration N_{ccn} and measured cloud microphysical properties N_{cd} and D_{eff}. A consistent, quantitative relationship among these variables would prove to be extremely useful for parameterizations of cloud properties based on aerosol properties. If N_{ccn} is found not to be the only controlling variable for these cloud properties, it is useful to identify and quantify these other relevant variables. A summary of the results from this section is found in Table 2.

4.5.1. Past studies. Few studies are available from which the relationship between N_{ccn} and cloud properties of marine stratus clouds can be quantitatively inferred. Hegg et al. (1991) measured airborne CCN spectra between 0.2 and 2% supersaturation off the coast of Washington State in and around marine stratus clouds, and cloud droplet concentrations using an FSSP-100. They found that N_{cd} is linearly related to N_{ccn} measured at 1% supersaturation according to $N_{cd} \sim 0.71 N_{ccn}$ with correlation coefficient R of 0.88. The reported

Table 2. *Summary of prior relationships among N_{ap}, N_{ccn}, N_{cd}, and D_{eff} and those for the present study; CI and R are the confidence interval and correlation coefficient, respectively*

Variables	Authors	Relationship	Notes
N_{ccn} versus N_{ap}	Bigg (1986)	Sublinear	95% CI: 0.32 to 0.58
	Raga and Jonas (1995)	$N_{ccn} \sim N_{ap}^{0.44}$	0.9% supersaturation
	Hegg et al. (1996)	$N_{ccn} \sim 0.1 N_{ap}$	Arctic location
	this study	$N_{ccn} \sim N_{ap}^{0.63}$	95% CI: 0.58 to 0.68
N_{ccn} versus predicted N_{ccn}	Liu et al. (1996)	$N_{ccn}/N_{ccn,predicted} = 0.9 \pm 0.3$	chemical data used
	Covert et al. (1998)	$N_{ccn}/N_{ccn,predicted} = 0.79$	90% of data between 0.6 and 1.1
			TDMA data used
N_{cd} versus N_{ccn}	Hegg et al. (1991)	$N_{cd} \sim 0.71 N_{ccn}$ (1% supersaturation)	clean air masses ($N_{ccn} < 80\ cm^{-3}$)
	Yum et al. (1998)	N_{cd} poorly correlated with N_{ccn}	$R \approx 0.3$
	this study	$N_{cd} \sim 0.71 N_{ccn}$ (0.1% supersaturation)	95% CI: 0.58 to 0.83
			$R = 0.9$
		or $N_{cd} \sim N_{ccn}^{0.31}$	95% CI: 0.24 to 0.38
			$R \approx 0.86$
D_{eff} versus N_{ccn}	Vong and Covert (1998)	$D_{eff} \sim -2.9 \ln N_{ap}$	$R = 0.72$
	this study	or $D_{eff} \sim -4.6 \ln N_{ccn}$ (derived)	derive using $N_{ccn} \sim N_{ap}^{0.63}$
		$D_{eff} \sim -4.2 \ln N_{ccn}$	95% CI: -3.5 to -4.9
			$R = 0.91$

data are, however, limited to relatively clean environments (maximum N_{cd} of 80 cm^{-3}).

Yum et al. (1998) compared CCN data acquired during the ACE-1 campaign (Hudson et al., 1998) with cloud droplet measurements obtained with an FSSP. They found that N_{cd} averaged over entire flights was poorly correlated ($R \simeq 0.3$) with cloud-base N_{ccn} at variety of supersaturations between 0.2 and 1.2%. Using an adiabatic parcel model with measured updraft velocities to predict N_{cd} from CCN data, the authors found greatly improved agreement between predicted and measured N_{cd}. Selection of air parcels that appeared to be near-adiabatic and not influenced by drizzle further improved the correlation. The apparent conclusion is that N_{cd} is a strong function of updraft velocity and therefore incorporation of this information greatly improves predicted N_{ccn}.

Twomey and Warner (1967) and Warner and Twomey (1967) compared cloud droplet concentrations with those derived from CCN measurements and an assumed updraft velocity of 3 m s^{-1} in cumulus clouds. They found fairly good agreement, especially at lower droplet concentrations.

4.5.2. Current study Because the *Pelican* and *Merlin* did not fly at exactly the same position at exactly the same time, the CCN data and cloud microphysical data are compared by averaging constant altitude legs from each. A typical flight was planned such that the *Pelican* and *Merlin* took off at approximately the same time so measurements made near takeoff were made very close in time. Because of the Merlin's faster speed and shorter flight duration, however the measurements became progressively separated in time. For the CLOUDYCOLUMN flights, the *Merlin* and *Pelican* average flight durations were 210 min and 340 min, respectively. The average time lag between *Pelican* CCN and *Merlin* FSSP measurements was approximately 60 min with a typical maximum lag of 100 min, although for very long *Pelican* flights the time difference was as much as 140 min. Furthermore, the *Pelican* flight plan typically consisted of multiple levels beneath cloud, usually including at least one near the ocean surface and one just under cloud. However, there is only one constant altitude leg of in-cloud data from the *Merlin* that is available that corresponds

to these multiple *Pelican* legs, so the average for each of these below-cloud legs is compared to the same in-cloud microphysical data set. Note that, as described above, it is believed that the 19 July N_{ccn} data are systematically low because of an instrument malfunction. In the following discussions we do not scale these data in any way, although such a scaling would cause only small changes in the quantitative relationships involving N_{ccn}.

Overall, the four flights for which complete data sets are available (07, 09, 16, and 19 July) can be separated into two categories: clean (16 and 19 July) and polluted (07 and 09 July). The N_{ccn} values encountered for both clean flights are approximately the same as can be seen from Fig. 7. This is also true for the two polluted cases with the exception of a single *Merlin* observation (which is compared to two *Pelican* observations at different altitudes). As a result, almost all of the data are grouped closely together with respect to N_{ccn}. Unfortunately, this prevents any meaningful examination of the functional relationship between N_{ccn} and N_{cd}, or N_{ccn} and D_{eff}, since any two-parameter function can be fit to the data. The relationships assumed in analyzing the data from this study, therefore, are guided by past observations.

Fig. 7 shows N_{cd} as a function of N_{ccn}. Overall, 33 observations were compiled from 103 min of in-cloud *Merlin* data and 13 h of *Pelican* below cloud data. The horizontal bars in Fig. 7 represent the standard deviation in N_{ccn} (which has a 60 s

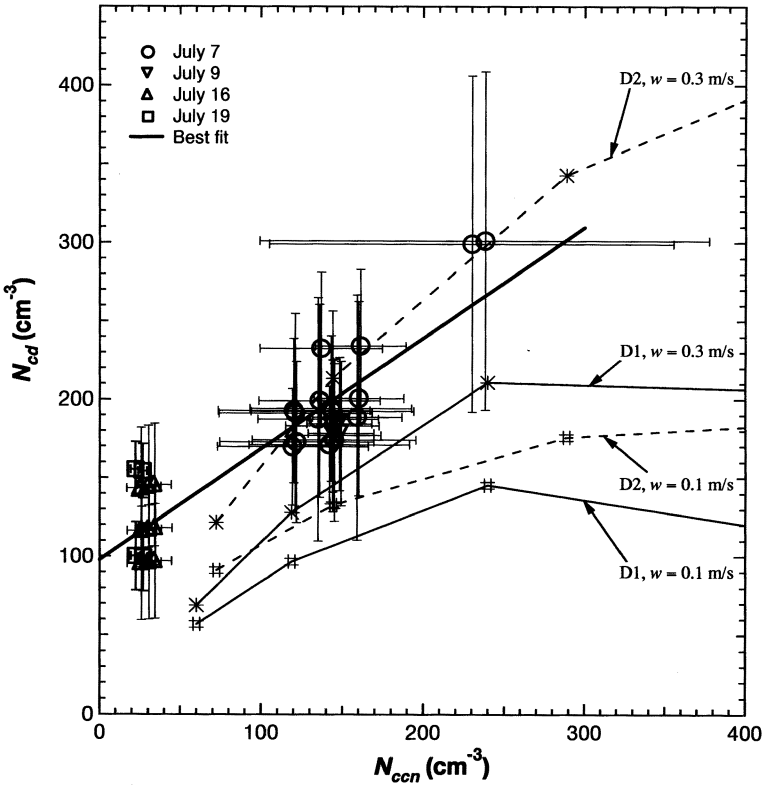

Fig. 7. Cloud droplet number concentration N_{cd} as a function of below-cloud CCN concentration at 0.1% supersaturation for the four CLOUDYCOLUMN flights. Model predictions (* and #, solid and dotted lines) correspond to two updraft velocities (0.1 and 0.3 m s^{-1}) and 2 aerosol size/chemical composition distributions (see Fig. 3 and text). The horizontal and vertical bars represent the standard deviation in the observations over the averaging period for each datum (see text). The symbols with lines are $N_{cd} - N_{ccn}$ relationships predicted by an adiabatic cloud parcel model for two different aerosol size distributions (D1 and D2) and two different updraft velocities w (0.1 and 0.3 m s^{-1}).

averaging time) for the observation period. The vertical bars represent the standard deviation in 30 s averaged N_{cd}. Regression of these data assuming a linear relationship (as per Hegg et al. (1991)) yields $N_{cd} \sim 0.71 N_{ccn}$ with an R value 0.9. The 95% confidence interval for the slope is 0.58 to 0.83. The fact that the slopes of the relationship between N_{cd} and N_{ccn} for the current study and for Hegg et al. (1991) are the same is at first surprising since the supersaturations for the CCN measurements were 0.1% and 1%, respectively. These two supersaturations correspond roughly to dry particle diameters of 0.1 μm and 0.03 μm for typical marine boundary layer aerosol. Both relationships cannot be true for identical cloud conditions unless there were no CCN between 0.1 and 1% supersaturation, which is clearly unrealistic. One possible explanation is that the effective supersaturation for stratus clouds during ACE-2 was significantly lower than that during the study of Hegg et al., resulting in similar fractions of 0.1% and 1% supersaturation CCN activating to form cloud droplets. The apparent similarity of the two studies would in such a case not be meaningful but coincidental.

As discussed above, a power-law relationship can just as easily be fitted to the data in Fig. 7 as a linear relationship since there are only two main groupings of data. A regression of these data using a power-law relationship yields $N_{cd} \sim N_{ccn}^{0.31}$, with an R value of 0.86 and a 95% confidence interval for the exponent of 0.24 to 0.38. It will be argued later that a power law is a more physically realistic relationship for these two variables and, therefore, should be more useful for relating N_{cd} to N_{ccn}.

4.5.3. Effective diameter. Fig. 8 shows D_{eff} as a function of N_{ccn}. Again, the horizontal and vertical bars represent the standard deviation in the 30 s and 60 s averaged D_{eff} and N_{ccn} data, respectively. A best-fit curve for the data plotted using a linear scale for D_{eff} and a log scale for N_{ccn} (as per Vong and Covert, (1998)) gives the relationship $D_{eff} \sim -4.2 \ln N_{ccn}$, $R = 0.91$, where D_{eff} is in μm and N_{ccn} in cm^{-3}. The 95% confidence interval for the slope is -3.5 to -4.9. For comparison, the data from Vong and Covert follows the relationship $D_{eff} \sim -2.9 \ln N_{ap}$, $R = 0.72$. If one uses the best-fit relationship $N_{ccn} \sim N_{ap}^{0.63}$, which is calculated for the present study using the same data set as Fig. 6 but without use of the chemical composition data, to convert the Vong and Covert data to CCN data their relationship becomes $D_{eff} \sim -4.6 \ln N_{ccn}$, which is similar to the slope obtained from this study. This similarity suggests that there might exist a consistent relationship between D_{eff} and N_{ccn} in stratus clouds, although more data are required to evaluate this possibility. It is important to note that D_{eff} has been predicted by adiabatic parcel models to depend strongly on cloud height, defined as the vertical distance above cloud base. Ideally, measurements used for determining the relationship between D_{eff} and N_{ccn} would be made at constant cloud height. A comparison of N_{ccn} with D_{eff} for samples at a variety of cloud heights, as is the case for the present study, would not be expected to result in a single curve, but rather a family of curves, each representing the relationship between D_{eff} and N_{ccn} at different cloud heights. Since the data from the present study are used to predict changes in D_{eff} (rather than its absolute value) as a function of N_{ccn}, it is plausible that the best-fit curve for these data is independent of the variability caused by these sampling complications, and therefore represents the dependency of D_{eff} on N_{ccn} if sampling were accomplished at constant cloud height. However, there is the possibility that D_{eff} was not uniformly sampled from all cloud heights which would cause a bias in the calculated relationship between D_{eff} and N_{ccn}.

Vong and Covert (1998) did not give a theoretical justification for their choice of relating D_{eff} to $\ln N_{ccn}$. Martin et al. (1994) suggest that an appropriate parameterization of effective diameter is $D_{eff} \sim (LWC/N_{cd})^{1/3}$. Assuming that to first order LWC is constant, and that N_{ccn} and N_{cd} are related linearly as found by Hegg et al. (1991), this relationship becomes $D_{eff} \sim N_{ccn}^{-0.33}$. If the data from the present study are also fitted to a power law, the result is the relationship $D_{eff} \sim N_{ccn}^{-0.27}$, with $R = 0.91$ and 95% confidence interval for the exponent of -0.22 to -0.32. If the data from Vong and Covert are similarly analyzed, the result is also $D_{eff} \sim N_{ccn}^{-0.27}$, with $R = 0.71$ and 95% confidence interval for the exponent of -0.23 to -0.30. Although not conclusive, the data from both Vong and Covert and the present study do support the scaling of D_{eff} and N_{cd} for the parameterization proposed by martin et al. (1994). In contrast, Moeng and Curry (1990) and McFarlane et al. (1992) proposed parameterizations that were

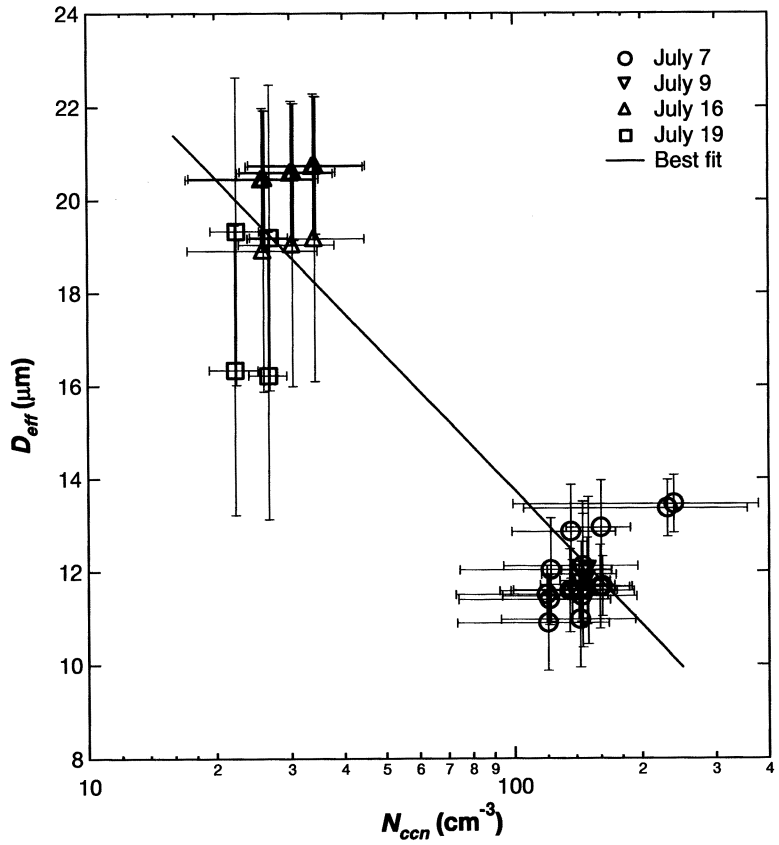

Fig. 8. Effective diameter of cloud droplets as a function of the below-cloud CCN concentration at 0.1% supersaturation for the four CLOUDYCOLUMN flights. The horizontal and vertical bars represent the standard deviation in the observations over the averaging period for each datum (see text).

dependent only on LWC and not directly dependent on N_{cd}. However, it seems reasonable that for clouds with the same LWC but different N_{cd}, D_{eff} would not necessarily be a constant as calculated by the latter two studies.

4.6. *Below cloud aerosol number concentration versus cloud droplet number concentration*

4.6.1. Past studies. Because many more studies address the relationship between accumulation mode aerosol number concentration N_{ap} and cloud droplet number concentration N_{cd} than between N_{ccn} and N_{cd}, these data will also be presented here and compared with previous work. Table 3 shows a summary of the conditions under which previous investigators have examined this relationship. In general, the methods for measuring N_{ap} and N_{cd} are similar although the variations in the size range measured could produce systematic biases in the data, as will be discussed shortly. The data from Pueschel et al. (1986) and Raga and Jonas (1993) are obtained from Slingo and Schwartz (1996), who replotted the data from both studies.

Fig. 9 shows the results from the studies listed in Table 3. The concentrations under the N_{cd} and N_{ap} columns give the approximate range of these variables over the various studies. Fitting all the data together (a total of 185 observations), assuming a straight line in log–log coordinates, gives the relationships $N_{cd} \sim N_{ap}^{0.48}$, $R = 0.75$, with a 95% confidence interval for the exponent of 0.42 to 0.55. The average value of $N_{cd,measured}/N_{cd,predicted}$ where $N_{cd,predicted}$ is obtained from the

Table 3. *Summary of studies of cloud droplet number concentration versus below-cloud or in-cloud aerosol accumulation mode number concentration*

Authors	Location	Cloud type	Platform	N_{ap}	N_{cd}
Pueschel et al. (1986) (from Slingo and Schwartz, 1996)	Whiteface Mtn, VT	continental strata	ground	0.1 to 47 μm 100 to 10 000 cm^{-3} in-cloud, ambient RH	0.5 to 47 μm 20 to 4000 cm^{-1}
Raga and Jonas (1993) (from Slingo and Schwartz, 1996)	British Isles	marine stratus	airborne	0.1 to 3 μm 50 to 5000 cm^{-3} below cloud, dry	2 to 47 μm 20 to 150 cm^{-3}
Martin et al. (1994)	California coast S. Atlantic British Isles N. Atlantic (Azores)	marine stratus	airborne	0.1 to 3 μm 0 to 1500 cm^{-3} below cloud, dry	0.5 to 47 μm 0 to 500 cm^{-3}
Gillani et al. (1995)	Syracuse, NY	continental stratus	airborne	0.17 to 2 μm 160 to 1100 cm^{-3} in-cloud, dry	2 to 35 μm 0 to 1100 cm^{-3}
Leaitch et al. (1996)	Nova Scotia Canada	marine stratus	airborne	0.13 to 3 μm 50 to 2000 cm^{-3} out of cloud, dry	2 to 35 μm 50 to 400 cm^{-3}
Vong and Covert (1998)	Cheeka Peak, WA	marine stratus	ground	0.08 to 47 μm 0 to 1000 cm^{-3} in-cloud, dry	2 to 47 μm 0 to 800 cm^{-3}
this study	N. Atlantic (Canary Islands)	marine stratus	airborne (2 aircraft)	0.1 to 3 μm 80 to 2000 below cloud, dry	2 to 47 μm 90 to 300 cm^{-3}

regression relationship, is 1.1, with 95% of the data lying between 0.30 and 2.1. We therefore conclude that, based on a data set containing a number of different studies, the best-fit relationship for these data can, 95% of the time, predict cloud droplet concentration to within a factor of 3.3 (= 1/0.3). While most of these studies did not report error bars for the data, it is unlikely that all of the observed variability can be wholly accounted for by instrumental error. Factors such as updraft velocity, entrainment, mixing, coalescence, and aerosol chemical composition and size distribution shape are expected to also contribute to this variability.

There does not seem to be a clear bias due to differences in the smallest or largest sizes measured for determining N_{ap} and N_{cd}. Even though Pueschel et al. (1986) and Martin et al. (1994) defined N_{cd} as droplets larger than 0.5 μm diameter rather than 2 μm, as used by the other studies, there does not appear to be a systematic shift towards higher N_{cd} in their data relative to the scatter present in the data set as a whole. Similarly, Leaitch et al. (1996) defined N_{ap} to be those particles larger than 0.17 μm diameter rather than 0.1 μm, but no shift towards lower N_{ap} is evident. Although data from Vong and Covert (1998) might be expected to exhibit a shift to higher N_{ap} because they defined N_{ap} to be particles larger than 0.08 μm, the opposite is observed.

4.6.2. Current study. For an examination of the data from the current study, the comments that apply to comparing *Pelican* N_{ccn} and *Merlin* microphysical measurements apply here also. The data presented are averaged size distributions obtained for exactly the same periods as are used for the CCN comparisons. N_{ap} is defined as the number concentration of particles between 0.1 and 3 μm dry diameter.

Fig. 10 shows N_{cd} as a function of N_{ap}. A log–log relationship was found to be more appropriate

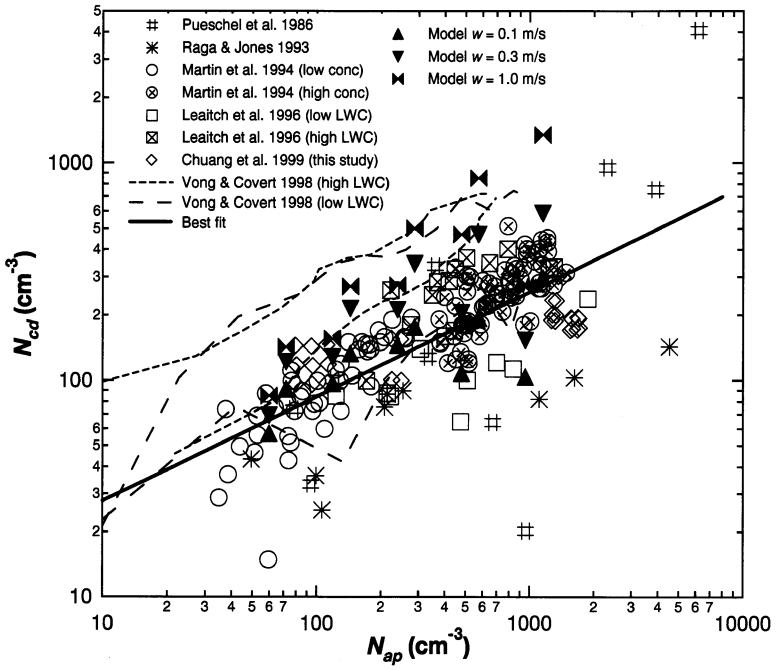

Fig. 9. Number concentration of cloud droplets as a function of below-cloud or in-cloud accumulation mode number concentration (as defined in Table 3 for each study) for the present study and data found from literature. The lines for the Vong and Covert (1998) data represent the envelope of their data (for both high and low liquid water content cases). The best fit line is a regression of all measurements except for the Vong and Covert data. The model data represents results for both size distributions D1 and D2.

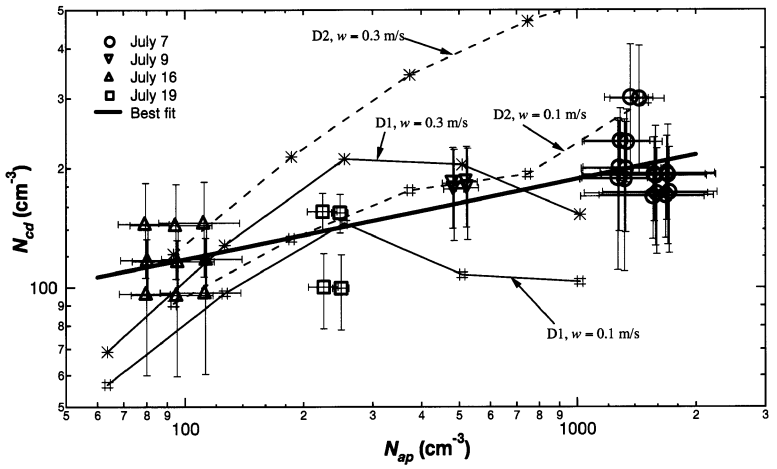

Fig. 10. Cloud droplet number concentration as a function of the accumulation mode aerosol concentration (defined as particles with dry $D_p > 0.1$ μm) for the four CLOUDYCOLUMN *Pelican* flights during ACE-2. The horizontal and vertical bars represent the standard deviation in the observations over the averaging period for each datum (see text). The symbols (* and #) with lines (solid and dotted) are N_{cd}–N_{ccn} relationships predicted by an adiabatic cloud parcel model for two different aerosol size distributions (D1 and D2) and two different updraft velocities ω (0.1 and 0.3 m s^{-1}).

than a linear relationship for these data. Regression of the data yields the relationship $N_{cd} \sim N_{ap}^{0.20}$ with $R = 0.80$ and 95% confidence interval for the exponent of 0.15 to 0.26. This exponent is significantly lower than the value of 0.48 that was found for a regression of all studies combined. In a study in the northeast Atlantic, Raga and Jonas (1993) do, however, find this exponent to be 0.25. Possible explanations for the lower value for the exponent observed here and by Raga and Jonas (1993) as compared with other studies include a consistently greater amount of entrainment or, perhaps, a systematic bias in updraft velocities. Entrainment would lead to a lower value for the exponent because it reduces the value of the maximum supersaturation attained in an air parcel, and as a result a smaller fraction of aerosol would activate to form cloud droplets. A systematically lower updraft velocity would also lead to a lower value of the exponent for the same reason.

4.7. *Discussion of N_{cd}, N_{ccn}, and N_{ap} relationships*

One expects a sublinear relationship between N_{cd} and N_{ccn} and therefore also between N_{cd} and N_{ap}. The latter assumes that N_{ap} and N_{ccn} are related either linearly or sublinearly as is consistent with previous studies and the present study. This expectation occurs because, for all variables held constant except the total number of CCN, an increase in N_{ccn} causes a suppression in the maximum supersaturation achieved in an air parcel that, in turn, should decrease the maximum critical supersaturation of the activated CCN. Therefore, the fraction of CCN that activate is reduced (for constant CCN spectrum) as the total number of CCN increases, resulting in a sublinear relationship between N_{cd} and N_{ccn}.

This effect is shown in Fig. 7 by the sublinear behavior of the adiabatic cloud parcel model predictions for two size distributions D1 and D2 and two updraft velocities (0.1 and 0.3 ms^{-1}). For both the predictions and measurements, the supersaturation at which N_{ccn} is determined is 0.1%, and N_{cd} is defined as those droplets greater than 2 μm diameter at cloud top. The predictions indicate that the slope of the relationship between N_{cd} and N_{ccn} is dependent on both updraft velocity and size distribution shape. Note that cloud thickness was assumed to be 100 m; changing the cloud thickness did not significantly change the predicted relationship between N_{cd} and N_{ccn} and between N_{cd} and N_{ap}. The best fit curve for the ACE-2 measured data agrees fairly well with the predictions for a cloud with an updraft velocity of 0.3 $m\,s^{-1}$, a reasonable value for marine stratus clouds. The variability in the measured data is comparable to that caused by the different size distributions considered or reasonable variations ($\sim$0.1 $m\,s^{-1}$) in the updraft velocity. The ability of the predictions to describe the qualitative features of the data may indicate that entrainment was not significant in the observed clouds since entrainment was not included in the adiabatic parcel model. We conclude that, while there is a consistent, quantitative relationship between N_{cd} and N_{ccn}, the actual relationship depends on other factors such as updraft velocity and the shape of the aerosol size distribution. This conclusion is consistent with the findings of Yum et al. (1998). Therefore, an important conclusion is that knowledge of N_{ccn} is useful and probably necessary for predicting cloud properties, but it is not sufficient for doing so accurately.

The model predictions also describe qualitatively observed relationships between N_{cd} and N_{ap} (Fig. 10), although not as well as that between N_{cd} and N_{ccn} (Fig. 7). The agreement in Fig. 10 is similar for updraft velocities for both 0.1 and 0.3 $m\,s^{-1}$, with the exception of the predictions using distribution D2 and updraft velocity of 0.3 $m\,s^{-1}$. The decrease of predicted N_{cd} at large N_{ap} for aerosol size distribution D1 results from the definition of N_{cd} as those droplets greater than 2 μm diameter. The depletion of water due to increasing N_{ap} shifts the droplet size distribution to sufficiently smaller sizes such that, for N_{ap} larger than 250 cm^{-3}, N_{cd} decreases with increasing N_{ap}. When droplets as small as 1 μm are included in N_{cd}, the curves monotonically increase like those from distribution D2. With this modification, the predictions for an updraft velocity of 0.1 $m\,s^{-1}$ more accurately match the observations of Fig. 10. Again, however, it should be noted that updraft velocity and size distribution shape can affect the relationship between N_{cd} and N_{ap}.

Comparing the predictions with the overall data set of N_{cd} versus N_{ap} (Fig. 9) shows good agreement for model updraft velocities of 0.1 and 0.3 $m\,s^{-1}$, and poorer agreement at 1 $m\,s^{-1}$ updraft velocity. This behavior is not unexpected

since the latter value is probably too high for typical marine stratus clouds. Variability in the predictions resulting from assumed updraft velocity is quite high, and is roughly the same magnitude as the scatter in the overall data set. This finding suggests that at least some of the variability of the data in Fig. 9 might be attributable to sampling of clouds formed from air with varying updraft velocity. The magnitude of these variations seems well within that expected for marine stratus cloud conditions. Changes in the size distribution shape do not appear to be as significant as changes in updraft velocity for the two distributions and the two updraft velocities considered here. However, these two size distributions do not reflect the range of distributions that can be found in the marine boundary layer; this study cannot rule out the possibility that the range of natural size distributions could cause variability in the relationship between N_{cd} and N_{ap} that is comparable to that caused by natural variations in updraft velocity. Therefore, we conclude that N_{ap}, similarly to N_{ccn}, can be used for predicting N_{cd}, but that other variables, specifically the shape of the aerosol number size distribution and the updraft velocity, must also be incorporated to improve such predictions.

5. Summary

CCN concentration at 0.1% supersaturation was measured onboard the CIRPAS *Pelican* using the Caltech CCN instrument in the northeast Atlantic during ACE-2. In general, the Caltech CCN data agree well with the University of Wyoming and MRF CCN instruments for periods when the instruments were measuring the same air mass. The CCN concentration data are consistent with similar measurements in clean marine conditions from previous studies.

A local CCN closure experiment was conducted. Local closure for CCN was not achieved, since a sublinear relationship between measured and derived CCN concentration, $N_{ccn} \sim N_{ccn,predicted}^{0.51}$, rather than a linear 1:1 relationship, best fits the data. This result is consistent with those of some previous studies based upon thermal diffusion cloud chamber measurements (Bigg, 1986; Raga and Jonas, 1995) but inconsistent with observations made using an isothermal haze chamber (Liu et al., 1996). Significant variability in the ratio of measured to predicted N_{ccn} was observed. This ratio lies between 0.09 and 0.89 for 95% of the data, suggesting that predictions of N_{ccn} using aerosol size distribution and chemical composition information as in the present study agree with measured values to within a factor of 11. The variability with respect to the best-fit relationship is also high, leading to the conclusion that 95% of the data lies within a factor of 2.4 of the best-fit prediction. About 80% of this variability is estimated to result from instrument error, with the remaining is unaccounted for. The observed sublinear behavior and large variability may not be a property of the aerosols but rather could be a result of instrumentation limitations. If, however, these observations are real phenomena, they suggest that additional variables may need to be considered in order to accurately and precisely predict CCN measurements. Further studies of CCN closure are required before any definitive conclusions regarding this important issue can be made. Improvements in instrumentation, particularly those that quantitatively measure time- and size-resolved aerosol chemical composition, would be particularly helpful towards this end. Quantitative, single-particle chemical composition information would be ideal for CCN closure experiments, but such technology is not currently available. An improved CCN closure experiment would involve size-resolved inorganic and organic (both insoluble and soluble) speciation (presently achieved using filter samples and therefore having inherently long averaging times, typically on the order of a few hours), along with real-time or near real-time chemical composition measures, such as humidified TDMA, which would allow monitoring of the temporal variation of aerosol chemical composition. Improvements in CCN instruments may prove to be the most valuable technological advance for the purpose of local CCN closure.

Measured relationships between N_{cd} and N_{ccn}, and N_{cd} and N_{ap} can be reasonably reproduced by adiabatic parcel model predictions assuming typical size and chemical composition distributions measured in the northeast Atlantic and for typical marine stratus updraft velocities. While these quantitative relationships appear to be a good starting point for parameterizing cloud properties, specifically N_{cd}, model predictions show that updraft velocity and the shape of the CCN

spectrum or aerosol size distribution are also important controlling variables and must be taken into account for these parameterizations to be accurate. Model predictions relating N_{cd} with N_{ap} are also consistent with the overall data set compiled from all available literature, although a large amount of variability is observed with respect to the best-fit curve $N_{cd} \sim N_{ap}^{0.48}$. This relationship predicts N_{cd} from N_{ap} to within a factor of 3.3 for 95% of the data. It is likely that some, but not all, of this variability can be accounted for by instrument error. Other factors such as chemical composition, activation kinetics, surface tension modification, and soluble gases may contribute significantly to the remaining observed variations.

The relationship between D_{eff} and N_{ccn} found for this study agrees with the only study found in the literature (Vong and Covert, 1998). The result appears to be consistent with the parameterization of D_{eff} proposed by Martin et al. (1994), and not with those proposed by Moeng and Curry (1990) and McFarlane et al. (1992).

6. Acknowledgements

This research is a contribution to the International Global Atmospheric Chemistry (IGAC) Core Project of the International Geosphere-Biosphere Programme (IGBP) and is part of the IGAC Aerosol Characterization experiments (ACE). Primary funding for this work has been provided by the National Science Foundation Grant ATM-9614105, and by the Office of Naval research Grant N00014-91-0119. The authors would also like to thank Athanasios Nenes for providing the adiabatic parcel model calculations, and Bob Charlson and Tad Anderson for their insightful comments and suggestions.

REFERENCES

Bigg, E. K. 1986. Discrepancy between observation and prediction of concentrations of cloud condensation nuclei. *Atmos. Res.* **20**, 81–86.

Bluth, R. T., Durkee, P. A., Seinfeld, J. H., Flagan, R. C., Russell, L. M., Crowley, P. A. and Finn, P. 1996. Center for interdisciplinary remotely-piloted aircraft studies (CIRPAS). *Bull. Am. Meteorol. Soc.* **77**, 2691–2699.

Brenguier, J. L., Bourrianne, T., Coelho, A. D., Isbert, J., Peytavi, R. Trevarin, D. and Weschler, P. 1998. Improvements of droplet size distribution measurements with the Fast-FSSP (Forward Scattering Spectrometer Probe). *J. Atmos. Ocean Technol.* **15**, 1077–1090.

Brenguier, J. L., Chuang, P. Y., Fouquart, Y., Johnson, D. W., Parol, F., Pawlowska, H. H., Pelon, J., Schüller, L., Schröder, F. and Snider, J. R. 2000. An overview of the ACE-2 CLOUDYCOLUMN closure experiment. *Tellus* **52B**, 815–827.

Cachier, H., Buat-Ménard, P., Fontugne, M. and Chesselet, R. 1986. Long-range transport of continentally-derived particulate carbon in the marine atmosphere: evidence from stable carbon isotope studies. *Tellus* **38B**, 161–177.

Charlson, R. J., Schwartz, S. E., Hales, J. M., Cess, R. D., Coakley, J. A., Hansen, J. E. and Hofmann, D. J. 1992. Climate forcing by anthropogenic aerosols. *Science* **255**, 423–430.

Chuang, P. Y., Charlson, R. J. and Seinfeld, J. H. 1997. Kinetic limitations on droplet formation in clouds. *Nature* **390**, 594–596.

Clarke, A. D., Porter, J. N., Valero, F. P. J. and Pilewskie, P. 1996. Vertical profiles, aerosol microphysics, and optical closure during the Atlantic stratocumulus transition experiment: measured and modeled column optical-properties. *J. Geophys. Res.* **101**, 4443–4453.

Collins, D. R., Jonsson, H. H., Seinfeld, J. H., Flagan, R. C., Gassó, S., Hegg, D. A., Russell, P. B., Schmid, B., Livingston, J. M., Öström, E., Noone, K. J., Russell, L. M. and Putaud, J. P. 2000. In-situ aerosol size distributions and CLEARCOLUMN radiative closure during ACE-2. *Tellus* **52B**, 498–525.

Covert, D. S., Gras, J. L., Wiedensohler, A. and Stratmann, F. 1988. Comparison of directly measured CCN with CCN modeled from the number-size distribution in the marine boundary layer during ACE 1 at Cape Grim, Tasmania. *J. Geophys. Res.* **103**, 16597–16608.

Delene, D. J., Deshler, T., Wechsler, P. and Vali, G. A. 1998. A balloon-borne cloud condensation nuclei counter. *J. Geophys. Res.* **103**, 8927–8934.

Hegg, D. A., Hobbs, P. V., Gassó, S., Nance, J. D. and Rangno, A. L. 1996. Aerosol measurements in the Arctic relevant to direct and indirect radiative forcing. *J. Geophys. Res.* **101**, 23349–23363.

Hegg, D. A. Radke, L. F. and Hobbs, P. V. 1991. Measurements of Aitken nuclei and cloud condensation nuclei in the marine atmosphere and their relation to the DMS–cloud–climate hypothesis. *J. Geophys. Res.* **96**, 18727–18733.

Hoppel, W. A., Twomey, S. and Wojciechowski, T. A. 1979. A segmented thermal diffusion chamber for continuous measurements of CN. *J. Aerosol Sci.* **10**, 369–373.

Hudson, J. G. 1989. An instantaneous CCN spectrometer. *J. Atmos. Ocean Technol.* **6**, 1055–1065.

Hudson, J. G. and Frisbie, P. R. 1991. Cloud condensation nuclei near marine stratus. *J. Geophys Res.* **96**, 20795–20808.

Hudson, J. G., Xie, Y. H. and Yum, S. S. 1998. Vertical distributions of cloud condensation nuclei spectra over the summertime Southern Ocean. *J. Geophys. Res.* **103**, 16609–16624.

Laaksonen, A., Korhonen, P., Kulmala, M. and Charlson, R. J. 1998. Modification of the Köhler equation to include soluble trace gases and slightly soluble substances. *J. Atmos. Sci.* **55**, 853–862.

Laktionov, A. G. 1972. A constant-temperature method of determining the concentrations of cloud condensation nuclei. *Atmos. and Oceanic Phys.* **8**, 672–677.

Liu, P. S. K., Leaitch, W. R., Banic, C. M., Li, S. M., Ngo, D. and Megaw, W. J. 1996. Aerosol observations at Chebogue Point during the 1993 North Atlantic Regional Experiment: relationships among cloud condensation nuclei, size distribution, and chemistry. *J. Geophys. Res.* **101**, 28971–28990.

Martin, G. M., Johnson, D. W. and Spice, A. 1994. The measurement and parameterization of effective radius of droplets in warm stratocumulus clouds. *J. Atmos. Sci.* **51**, 1823–1842.

McFarlane, N. A., Boer, G. J., Blanchet, J.-P. and Lazare, M. 1992. The Canadian Climate Centre second-generation general circulation model and its equilibrium climate. *J. Climate* **5**, 1013–1044.

Moeng, C.-H. and Curry, J. 1990. The sensitivity of large eddy simulations of a stratus topped boundary layer to cloud microphysics. In *Proc. Conf. on Cloud Physics*, pp. 115–121. San Francisco, Amer. Meteor. Soc.

O'Dowd, C. D., Smith, M. H., Consterdine, I. E. and Lowe, J. A. 1997. Marine aerosol, sea-salt and the marine sulphur cycle: a short review. *Atmos. Env.* **31**, 73–80.

Pueschel, R. F., Vanvalin, C. C., Castillo, R. C., Kadlecek, J. A. and Ganor, E. 1986. Aerosols in polluted versus nonpolluted air masses — long-range transport and effects on clouds. *J. Clim. Appl. Meteorol.* **25**, 1908–1917.

Putaud, J. P., Dingenen, R. V., Mangoni, M., Virkkula, A., Raes, F., Maring, H., Prospero, J., Swietlicki, E., Berg, O., Hillamo, R. and Makela, T. 2000. Chemical mass closure and origin assessment of the submicron aerosol in the marine boundary layer and the free troposphere at Tenerife during ACE-2. *Tellus* **52B**, 141–168.

Raga, G. B. and Jonas, P. R. 1993. On the link between cloud-top radiative properties and sub-cloud aerosol concentrations. *Q. J. R. Meteorol. Soc.* **119**, 1419–1425.

Raga, G. B. and Jonas, P. R. 1995. Vertical distribution of aerosol particles and CCN in clear air around the British Isles. *Atmos. Env.* **29**, 673–684.

Russell, L. M., Zhang, S. H., Flagan, R. C., Seinfeld, J. H., Stolzenburg, M. R. and Caldow, R. 1996. Radially classified aerosol detector for aircraft-based submicron aerosol measurements. *J. Atmos. Ocean Technol.* **13**, 598–609.

Shulman, M. L., Jacobson, M. C., Charlson, R. J., Synovec, R. E. and Young, T. E. 1996. Dissolution behavior and surface tension effects of organic compounds in nucleating cloud droplets. *Geophys. Res. Lett.* **23**, 603–603.

Slingo, A. and Schwartz, S. E. 1996. Enhanced shortwave cloud radiative forcing due to anthropogenic aerosols. In P. J. Crutzen and V. Ramanathan (eds.), *Clouds, chemistry and climate*, pp. 191–236. Springer-Verlag.

Twomey, S. 1963. Measurements of natural cloud nuclei *J. Rech. Atmos.* **1**, 101–105.

Twomey, S. 1977. *Atmospheric aerosols.* Elsevier.

Twomey, S. and Warner, J. 1967. Comparison of measurements of cloud droplets and cloud nuclei. *J. Atmos. Sci.* **24**, 702–703.

Twomey, S. and Wojciechowski, T. A. 1969. Observations of the geographical variation of cloud nuclei. *J. Atmos. Sci.* **26**, 694–688.

Vong, R. J. and Covert, D. S. 1998. Simultaneous observations of aerosol and cloud droplet size spectra in marine stratocumulus. *J. Atmos. Sci.* **55**, 2180–2192.

Warner, J. and Twomey, S. 1967. The production of cloud nuclei by cane fires and the effect on cloud droplet concentration. *J. Atmos. Sci.* **24**, 704–706.

Yum, S. S., Hudson, J. G. and Xie, Y. H. 1998. Comparisons of cloud microphysics with cloud condensation nuclei spectra over the summertime Southern Ocean. *J. Geophys. Res.* **103**, 16625–16636.

Zhang, S. H., Akutsu, Y., Russell, L. M., Flagan, R. C. and Seinfeld, J. H. 1995. Radial differential mobility analyzer. *Aerosol Sci. Technol* **23**, 357–372.